Resonant scattering of light in a near-black-hole metric

Y. V. Stadnik, G. H. Gossel, V. V. Flambaum, and J. C. Berengut
School of Physics, University of New South Wales, Sydney 2052, Australia
(Dated: October 29, 2012)

We show that low-energy photon scattering from a body with radius R slightly larger than its Schwarzschild radius r_s resembles black-hole absorption. This absorption occurs via capture to one of the many long-lived, densely packed resonances that populate the continuum. The lifetimes and density of these meta-stable states tend to infinity in the limit $r_s \to R$. We determine the energy averaged cross-section for particle capture into these resonances and show that it is equal to the absorption cross-section for a Schwarzschild black hole. Thus, a non-singular static metric may trap photons for arbitrarily long times, making it appear completely 'black' before the actual formation of a black hole.

PACS numbers: 04.62.+v, 04.70.Dy, 04.70.-s

I. INTRODUCTION

In this work, we consider the scattering of photons by the gravitational field of a non-rotating, finite-sized body. Such finite-sized bodies have radius R that slightly exceeds their Schwarzschild radius $r_s = 2GM/c^2$. We show that low-energy photon scattering from such objects resembles black hole absorption. The absorption arises due to the existence of a dense spectrum of narrow resonances (meta-stable states) whose lifetime and density tend to infinity in the limit $r_s \to R$.

Photons captured to such a resonant state are trapped on the interior of the body for a time $t \sim \hbar/\Gamma_n$, where Γ_n is the width of a given resonance. For $r_s \to R$, both the energy spacing D and width Γ_n tend to zero ($t \to \infty$), while their ratio remains finite. This allows us to define the total cross-section for particle capture into these long-lived states using the optical model [1], which is calculated by averaging over a small energy interval containing many resonances. At low energy the resonance capture cross-section is $\sigma_a = 4\pi\varepsilon^2 r_s^4/3$ where ε is the energy of the incident particle. The absence of a longitudinal mode for photons means there is no state with total angular momentum equal to zero, hence the above cross-section tending to zero for zero energy.

This cross-section exactly matches the absorption cross-section for a Schwarzschild black hole calculated by assuming complete absorption at the event horizon (see Refs. [2–8]) derived previously for massless spin-1 particles [9, 10]. Note, however, that our calculation does not impose any special conditions at the boundary. Thus by considering the purely elastic cross-section of low-energy incident photons, we find that the absorption properties of a body with $r_s \to R$ resemble those of a black hole.

The gravitational field of these near-black-hole objects is described using a suitable metric to model the interior, which is then joined to the standard Schwarzschild exterior metric at the boundary of the body. The above result is shown to be valid for any interior metric satisfying the following conditions: continuity with the Schwarzschild exterior at $r = R$, a potential that deepens and develops a singularity in the black hole limit (allowing the particle to be treated semi-classically) and that this potential can be modeled as a harmonic oscillator in some finite region around the origin. We expect these conditions to be met by a large class of metrics; in this paper we present two metrics for which these conditions hold.

Additionally, the results presented include the spin-0 (scalar) case considered previously (for $j = 0$) [11], but given here for arbitrary angular momentum j. In this case taking $r_s \to R$ once again yields the black hole absorption cross-section given in [4].

For a more detailed discussion of previous calculations involving scattering of various particles in the black hole spacetime we turn the readers attention to the introductions in [7, 11] and references therein. As in previous work [11] we perform both analytical and numerical calculations, with good agreement between the two.

II. WAVE EQUATIONS

The Klein-Gordon equation for a massless spin-0 particle on a curved manifold (with $\hbar = c = 1$) reads

$$\partial_\mu(\sqrt{-g}g^{\mu\nu}\partial_\nu\Psi) = 0. \tag{1}$$

For massless spin-1 particles (photons) Maxwell's equations on a curved manifold free of charges read

$$\partial_\beta(\sqrt{-g}F^{\alpha\beta}) = 0, \tag{2}$$

where $F^{\alpha\beta} = \partial^\alpha A^\beta - \partial^\beta A^\alpha$ and A^μ is the contravariant electromagnetic 4-potential. One may write a general static, spherically symmetric metric in the form

$$ds^2 = -e^{\nu(r)}dt^2 + e^{\lambda(r)}dr^2 + r^2 d\Omega^2. \tag{3}$$

By applying the separation of variables

$$\Psi = e^{-i\varepsilon t}\phi(r)\,Y_{jm}(\theta,\varphi)$$
$$A_\varphi = e^{-i\varepsilon t} r\phi(r)\sin\theta\,\frac{dP_j(\cos\theta)}{d\theta}$$

to (1) and (2) respectively in the metric (3), one derives at the radial differential equations for spin-0 and spin-1

respectively. In the latter we have implemented a gauge such that A_φ is the only non-zero component [12].

Defining s as the particle spin, either 0 or 1, the radial equations for both spins can be combined to yield

$$\frac{d^2\phi}{dr^2} + \left[\left(\frac{\nu' - \lambda'}{2}\right) + \frac{2}{r}\right]\frac{d\phi}{dr} + \left[e^{\lambda-\nu}\varepsilon^2 + s^2\left(\frac{\nu' - \lambda'}{2r}\right) - \frac{j(j+1)e^\lambda}{r^2}\right]\phi(r) = 0, \quad (4)$$

where j the total angular momentum such that $j - s \geq 0$.

III. GENERAL INTERIOR SOLUTION

Equation (4) can be transformed into a Schrödinger-like equation by making the substitution $\phi(r) = \chi(r)/r$ and then mapping the radial coordinate to the Regge-Wheeler "tortoise" coordinate r^* defined by $dr^* = e^{(\lambda-\nu)/2}dr$. This gives us

$$\chi''(r^*) + \left[\varepsilon^2 + \frac{(s^2-1)}{2r}\frac{d}{dr}e^{\nu(r)-\lambda(r)} - \frac{j(j+1)e^{\nu(r)}}{r^2}\right]\chi(r^*) = 0. \quad (5)$$

For a near-black-hole interior metric, $e^{\nu(r)} \to 0$ for $0 \leq r \leq R$, as time slows down in the limit $r_s \to R$. This means that we may neglect all but the first term in square brackets in Eqn. (5) for all except very small energies. The solution regular at the origin is then $\chi(r^*) \simeq \sin(\varepsilon r^*)$. For $r_s \neq R$ there is still a non-zero contribution to Eqn. (4) from the potentially large $j(j+1)$ term. This can be accounted for by introducing φ as a constant phase shift determined by the boundary conditions at the origin (see below), giving

$$\chi(r) = \sin\left(\varepsilon\int_0^r e^{[\lambda(r')-\nu(r')]/2}dr' + \varphi\right), \quad (6)$$

which is now no longer regular at the origin, but is valid far from it.

For small r, the $j(j+1)$ term in Eqn. (4) dominates and gives rise to the standard centrifugal barrier term assuming that, for small r, $e^\nu \approx const$ and $e^\lambda \to 1$. These assumptions are valid for the specific metrics we consider in Sec IX, and apply to a larger class of static solutions where the potential is harmonic near the origin.

The phase shift induced by the centrifugal barrier, as computed far from the origin where the barrier is suppressed, is $-j\pi/2$. Therefore, we write the phase near the boundary $r \simeq R$ as

$$\Phi(r) = \varepsilon\int_0^r e^{\left[\lambda(r')-\nu(r')\right]/2}dr' - j\pi/2, \quad (7)$$

which is valid when the classical turning point $r_t \ll R$. Furthermore, at the boundary we have $\Phi'(R) = \varepsilon e^{(\lambda-\nu)/2} = \varepsilon R/(R - r_s)$. The latter is computed by imposing continuity of the metric at the boundary (where all but the energy term in Eqns. (4) and (5) are suppressed). Defining

$$\Lambda(r_s) = \int_0^R e^{(\lambda-\nu)/2}dr, \quad (8)$$

the logarithmic derivative of the interior wavefunction at $r = R$ can be written as

$$\left.\frac{\phi'(r)}{\phi(r)}\right|_R = \frac{\varepsilon R}{R - r_s}\cot\left[\varepsilon\Lambda(r_s) - j\pi/2\right] - \frac{1}{R}. \quad (9)$$

In the black-hole limit $e^\nu \to 0$, therefore from Eqn. (8) we see that as $r_s \to R$, $\Lambda(r_s)$ tends to infinity. In the quantum case this is because $\Lambda(r_s)$ is related (but not equal) to the total phase accumulated by the particle on the interior. This phase is large due to the wave function oscillating many times on the interior as the particle moves rapidly in the strong field. However this integral also gives the classical time that a massless particle ($ds^2 = 0$) spends on the interior, which goes to infinity in the black hole limit.

It is worth noting that the phase in Eqn. (7) evaluated at the boundary does *not* correspond to the total phase accumulated over the interior as this requires explicit knowledge of r_t.

However, the discrepancy with the total phase is only a constant offset in the limit $r_s \to 1$, and (7) gives rise to a good approximation to the wavefunction and its derivative at the boundary.

IV. GENERAL EXTERIOR SOLUTION

The metric on the exterior of a static massive body is given by the standard Schwarzschild metric, which yields the following radial differential equation

$$\frac{d^2\phi}{dr^2} + \left(\frac{1}{r - r_s} + \frac{1}{r}\right)\frac{d\phi}{dr} + \left[\frac{\varepsilon^2 r^2}{(r - r_s)^2} + \frac{s^2 r_s}{r^2(r - r_s)} - \frac{j(j+1)}{r(r - r_s)}\right]\phi(r) = 0. \quad (10)$$

A. Region I ($r \approx r_s$)

For $\varepsilon \ll (r - r_s)$ (later verified in our region of interest), Eqn. (10) becomes

$$\frac{d^2\phi}{dr^2} + \left(\frac{1}{r - r_s} + \frac{1}{r}\right)\frac{d\phi}{dr} + \left[\frac{s^2 r_s}{r^2(r - r_s)} - \frac{j(j+1)}{r(r - r_s)}\right]\phi(r) = 0, \quad (11)$$

which has the exact solution

$$\phi_{\rm I}(r) = \alpha_1 \left(\frac{r}{r_s}\right)^s P_{j-s}^{(2s,0)}\left(1-\frac{2r}{r_s}\right) + \beta_1 \left(\frac{r_s}{r}\right)^{j+1} {}_2F_1\left(j-s+1, j+s+1, 2j+2; \frac{r_s}{r}\right), \tag{12}$$

where $P_n^{(a,b)}(x)$ represent the Jacobi polynomials and ${}_2F_1(a,b,c;z)$ is the Gaussian hypergeometric function.

B. Region II ($r \gg r_s$)

In this region we assume low energy in Eqn. (10) as before and make the substitutions $\phi(r) = \chi(r)/r$ and $r = \rho/\varepsilon$. This yields

$$\frac{d^2\chi}{d\rho^2} + \left[1 + \frac{2\varepsilon r_s}{\rho} - \frac{j(j+1)}{\rho^2}\right]\chi = 0. \tag{13}$$

The corresponding solution in terms of the regular and irregular Coulomb wave functions reads

$$\phi_{\rm II}(r) = \frac{\alpha_2 F_j(\varepsilon r_s, \varepsilon r) + \beta_2 G_j(\varepsilon r_s, \varepsilon r)}{r}. \tag{14}$$

By matching the coefficients of (12) and (14) in the limits $r \gg r_s$ and $\varepsilon r \ll 1$ simultaneously, using the appropriate asymptotic forms of these solutions [13], we arrive at the following relationship between the coefficients of the solutions in Regions I and II as

$$\frac{\alpha_2}{\beta_2} = \frac{\alpha_1}{\beta_1}\frac{(2j)!(-1)^{j-s}}{(j-s)!(j+s)!C^2(2j+1)(\varepsilon r_s)^{2j+1}}, \tag{15}$$

$$C = \frac{2^j e^{\varepsilon r_s \pi/2}|\Gamma(j+1-i\varepsilon r_s)|}{(2j+1)!}.$$

V. S-MATRIX

The solution to Eqn. (10) at large distances can also be written in terms of outgoing and incoming waves as

$$\phi_{\rm II}(r) = \frac{A_j e^{iz} + B_j e^{-iz}}{r}, \tag{16}$$

where $z = \varepsilon r + \varepsilon r_s \ln(2\varepsilon r) + \delta_j^C - j\pi/2$ and $\delta_j^C = \arg[\Gamma(j+1+i\varepsilon r_s)]$ is the Coulomb phase shift. This allows us to write the scattering matrix as [1]

$$S_j = (-1)^{j+1}\frac{A_j}{B_j}e^{2i\delta_j^C}. \tag{17}$$

Imposing the condition $\varepsilon r \gg 1$ in Eqn. (14), we have the following asymptotic form of the wavefunction in region II

$$\phi_{\rm II}(r) = \frac{\alpha_2 \sin(z) + \beta_2 \cos(z)}{r}, \tag{18}$$

which, upon matching to (16), gives the scattering matrix as

$$S = -\frac{1-\frac{i\alpha_2}{\beta_2}}{1+\frac{i\alpha_2}{\beta_2}}e^{2i\delta_j^C}. \tag{19}$$

VI. MATCHING OF WAVEFUNCTIONS AT BOUNDARY AND RESONANCE ENERGIES

Matching the logarithmic derivatives of the exterior (12) and interior (9) wavefunctions at $r = R$ and taking the black hole limit $r_s \to R$ gives

$$\frac{\alpha_1}{\beta_1} = -\frac{(-1)^{s-j}\Gamma(2j+2)\tan(\varepsilon\Lambda(r_s) - j\pi/2)}{\varepsilon R\,\Gamma(j-s+1)\Gamma(j+s+1)}. \tag{20}$$

Resonances occur at energies where the absorption cross-section is maximized, i.e. $S = -1$. This is achieved in Eqn. (19) by setting $\alpha_2/\beta_2 = 0$, which by Eqn. (15) is equivalent to $\alpha_1/\beta_1 = 0$. Setting α_1/β_1 to zero in (20) results in the resonance condition for the energy

$$\varepsilon_n = \frac{n\pi + j\frac{\pi}{2}}{\Lambda(r_s)}, \tag{21}$$

where $n = 1, 2, \ldots$. Note that these resonance energies strongly depend on the value of j, but differ marginally between $s = 0$ and $s = 1$.

VII. RESONANCE WIDTHS

The full resonance condition corresponds to complex energies $\varepsilon = \varepsilon_n - i\Gamma_n/2$ for which the scattering matrix (19) has a complex pole. This occurs when

$$1 + \frac{i\alpha_2}{\beta_2} = 0. \tag{22}$$

On resonance $\alpha_1/\beta_1 = 0$ allowing us to expand this expression near $\varepsilon = \varepsilon_n$ as

$$\frac{\alpha_1}{\beta_1}(\varepsilon) = \left.\frac{\alpha_1}{\beta_1}\right|_{\varepsilon=\varepsilon_n} + \left.\frac{\partial}{\partial\varepsilon}\left(\frac{\alpha_1}{\beta_1}\right)\right|_{\varepsilon=\varepsilon_n}(\varepsilon - \varepsilon_n) \tag{23}$$

At the complex pole of the scattering matrix, $\varepsilon = \varepsilon_n - i\Gamma_n/2$, this gives

$$\frac{\alpha_1}{\beta_1} = \left.\frac{\partial}{\partial\varepsilon}\left(\frac{\alpha_1}{\beta_1}\right)\right|_{\varepsilon=\varepsilon_n}\left(\frac{-i\Gamma_n}{2}\right), \tag{24}$$

where we have only substituted for energy where it appears explicitly in Eqn. (23). Using (15), (20), (22) and (24) (with $\varepsilon \approx \varepsilon_n$, $r_s \to R$), the resonance widths are given by

$$\Gamma_{n,j} = \frac{2C^2(\varepsilon R)^{2j+2}((j-s)!)^2((j+s)!)^2}{((2j)!)^2\Lambda(r_s)}, \tag{25}$$

where we have assumed $\varepsilon\Lambda(r_s) \gg j\pi/2$, i.e. large n (see (21)), which is already assumed when invoking the semi-classical approximation.

VIII. ABSORPTION CROSS-SECTION

As discussed in Section III, in the black hole limit we find that $\Lambda(r_s)$ tends to infinity. Thus by Eqns. (21) and (25) both ε_n and Γ_n tend to zero in the limit $r_s \to R$ for any fixed, finite values of n and j. However, the ratio Γ_n/D remains constant, where $D = \varepsilon_{n+1} - \varepsilon_n$ is the spacing between adjacent levels. This allows us to use the optical-model (energy-averaged absorption cross-section) [1]. This is obtained by averaging over a small energy interval containing many resonances and reads

$$\bar{\sigma}_a^{\rm opt} = \sum_{j-s=0}^{\infty} \frac{2\pi^2}{\varepsilon^2}\frac{\Gamma_{n,j}}{D}(2j+1). \tag{26}$$

Substituting (21) and (25) into (26), gives

$$\bar{\sigma}_a^{\rm opt} = \sum_{j-s=0}^{\infty} \frac{4\pi(2j+1)C^2\varepsilon^{2j}R^{2j+2}((j-s)!)^2((j+s)!)^2}{((2j)!)^2}, \tag{27}$$

which is independent of $\Lambda(r_s)$ and thus of the interior metric.

By setting $s = 0$ or $s = 1$ in Eqn. (27) we recover the low-energy, total absorption cross-sections for massless scalar particles [4] or photons [9, 10], respectively, incident on a Schwarzschild black hole.

IX. SPECIFIC INTERIOR METRICS

In this section we present calculations involving two specific interior metrics that allow the $r_s \to R$ limit to be taken: the Florides [14] and Soffel [15] metrics. Specifically, we verify our analytic solutions with numerically calculated resonance widths and energies via the short range phase shift $\delta(\varepsilon)$. To calculate $\delta(\varepsilon)$ we solve the second-order differential equation (4) numerically, for given e^ν and e^λ, with the boundary condition $\phi(r \to 0) \sim r^j$ using *Mathematica* [16]. This solution provides a real boundary condition for the *exterior* wave function at $r = R$. (We set $R = 1$ in the numerical calculations). Equation (10) is then integrated outwards to large distances $r \gg r_s$. In this region Eq. (10) takes the form of a non-relativistic Schrödinger equation for a particle with momentum ε and unit mass in the Coulomb potential with charge $Z = -r_s\varepsilon^2$. Hence, we match the solution with the asymptotic form [1]

$$\chi(r) \propto \sin[\varepsilon r - (Z/\varepsilon)\ln 2\varepsilon r + \delta_C + \delta - j\pi/2] \tag{28}$$

and determine the short-range (numeric) phase shift δ. This phase possesses steps of height π at the resonance positions ε_n. We fit the step profile of an individual resonance to the Breit-Wigner function

$$\delta(\varepsilon \simeq \varepsilon_n) = \delta_n + \arctan\left[\frac{\varepsilon - \varepsilon_n}{\Gamma_n/2}\right] \tag{29}$$

where δ_n is a constant, from which we extract the numeric resonance widths and positions Γ_n and ε_n.

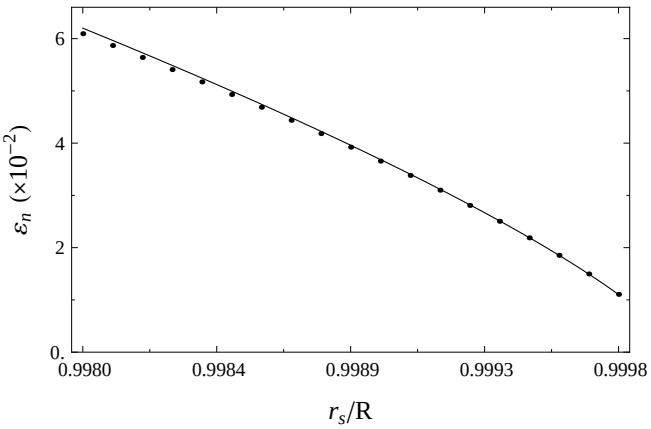

FIG. 1. Energies of the $n = 2$ resonance in the Florides metric with $s = j = 1$. Closed circles indicate numeric data, the solid line indicates analytic ε_n given by Eqn. (21) with $\Lambda(r_s)$ given by Eqn. (31).

A. Florides Interior

The Florides metric is characterized by

$$e^{\nu(r)} = \frac{(1-r_s/R)^{3/2}}{\sqrt{1-r_s r^2/R^3}}, \quad e^{\lambda(r)} = \left(1 - \frac{r_s r^2}{R^3}\right)^{-1}. \tag{30}$$

This in turn leads to

$$\begin{aligned}\Lambda(r_s)_{\rm F} &\overset{r_s \to R}{=} \frac{\pi^{3/2}R}{\sqrt{2}\Gamma(1/4)\Gamma(5/4)(1-r_s/R)^{3/4}} \\ &\approx 1.198\,(1-r_s/R)^{-3/4}.\end{aligned} \tag{31}$$

The resulting resonance energies and widths are compared with their numeric counterparts in Figures (1) and (2) respectively.

B. Soffel Interior

The Soffel metric is characterized by [15]

$$e^{\nu(r)} = \left(1 - \frac{r_s}{R}\right)\exp\left[-\frac{r_s(1-r^2/R^2)}{2R(1-r_s/R)}\right], \tag{32}$$

with $e^{\lambda(r)}$ equal to that of the Florides case. This in turn leads to

$$\Lambda(r_s)_{\rm So} \overset{r_s \to R}{=} R\sqrt{\pi}\exp\left[\frac{r_s/R}{4(1-r_s/R)}\right]. \tag{33}$$

Analytic and numeric ε_n and Γ_n for the Soffel metric are compared in Figures (3) and (4) respectively.

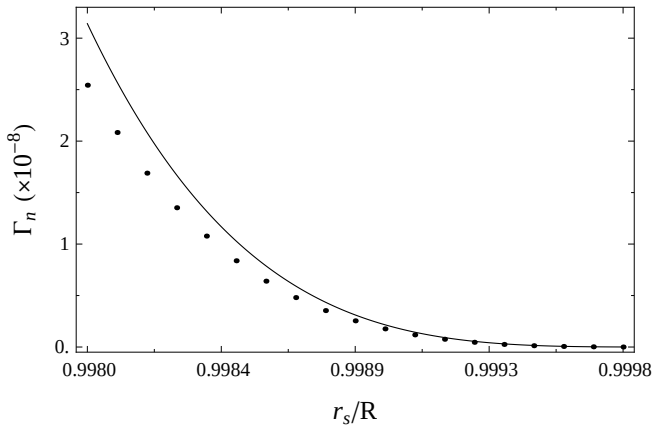

FIG. 2. Widths of the $n = 2$ resonance in the Florides metric with $s = j = 1$. Closed circles indicate numeric data, the solid line indicates analytic Γ_n given by Eqn. (25) with $\Lambda(r_s)$ given by Eqn. (31).

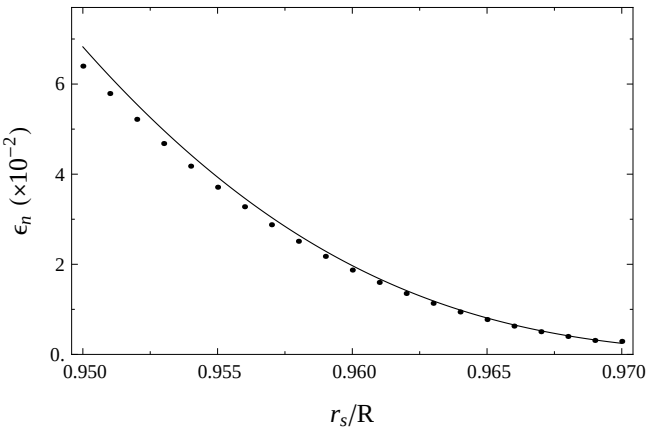

FIG. 3. Energies of the $n = 4$ resonance in the Soffel metric with $s = j = 1$. Closed circles indicate numeric data, the solid line indicates analytic ε_n given by Eqn. (21) with $\Lambda(r_s)$ given by Eqn. (33).

X. CONCLUSIONS

The problems of the scattering of low-energy, massless spin-0 and spin-1 particles from a massive, static, spherical body have been considered. We have shown that such scattering is characterized by a dense set of long lived resonances. Capture to these long-lived states gives rise to effective absorption in a purely potential scattering setting. In the black hole limit the cross-section for absorption exactly equals the cross-section in the pure black hole case (for low energy). Thus scattering of photons (and massless scalars) by a near-black-hole object resembles black hole absorption.

We thank G. F. Gribakin for useful discussions. This work is supported by the Australian Research Council.

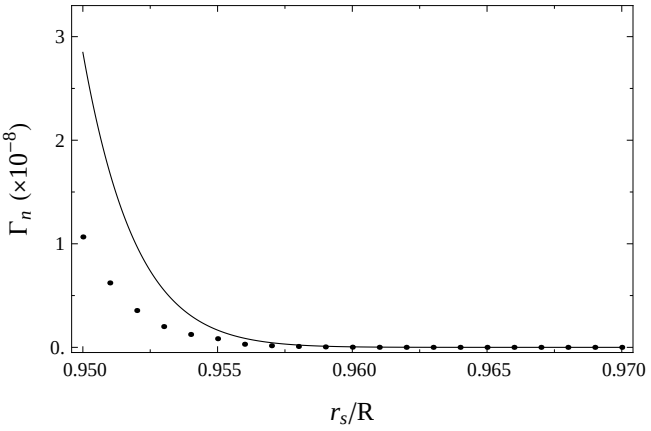

FIG. 4. Widths of the $n = 4$ resonance in the Soffel metric with $s = j = 1$. Closed circles indicate numeric data, the solid line indicates analytic Γ_n given by Eqn. (25) with $\Lambda(r_s)$ given by Eqn. (33).

[1] L. D. Landau and E. M. Lifshitz, *Quantum Mechanics*, 3rd Ed. (Butterworth-Heinemann, Oxford, 1977).
[2] R. A. Matzner, J. Math. Phys. **9**, 163 (1968).
[3] A. A. Starobinskii, Zh. Eksp. Teor. Fiz. **64**, 48 (1973) [Sov. Phys. JETP **37**, 28 (1973)].
[4] W. G. Unruh, Phys. Rev. D **14**, 3251 (1976); Thesis, Princeton Univ., 1971 (unpublished).
[5] N. Sanchez, Phys. Rev. D **18**, 1030 (1978).
[6] S. R. Das, G. Gibbons, and S. D. Mathur, Phys. Rev. Lett. **78**, 417 (1997).
[7] L. C. B. Crispino, S. R. Dolan, and E. S. Oliveira Phys. Rev. Lett. **102**, 231103 (2009).
[8] Y. Décanini, G. Esposito-Farèse, A. Folacci, Phys. Rev. D **83**, 044032 (2011).
[9] R. Fabbri, Phys. Rev. D **12**, 933, (1975).
[10] P. Kanti and J. March-Russell, Phys. Rev. D **67**, 104019, (2003).
[11] V. V. Flambaum, G. H. Gossel and G. F. Gribakin, Phys. Rev. D **85**, 084027 (2012).
[12] J. A. Wheeler. Geons. Phys. Rev., 97, 511, (1955).
[13] M. Abramowitz and I. A. Stegun, *Handbook of Mathematical Functions with Formulas, Graphs, and Mathematical Tables*, 10th Ed. (National Bureau of Standards, 1972).
[14] P. S. Florides, Proc. R. Soc. Lond. A **337**, 529 (1974).
[15] M. Soffel, B. Müller, and W. Greiner, J. Phys. A **10**, 551 (1977).
[16] *Mathematica, Version 7.0* (Wolfram Research, Inc., Champaign, IL, 2008).